npj | parkinson's disease

Article

Published in partnership with the Parkinson's Foundation

https://doi.org/10.1038/s41531-025-01179-6

The influence of intermittent hypercapnia on cerebrospinal fluid flow and clearance in Parkinson's disease and healthy older adults

Erik B. Erhardt[1], Andrew R. Mayer[2], Henry C. Lin[3,4], Sarah E. Pirio Richardson[3,5], Nicholas A. Shaff[2], Andrei A. Vakhtin[2], Arvind Caprihan[2], Harm J. van der Horn[2,6], Natalie Hoffman[2], John P. Phillips[2], Madeleine Grigg-Damberger[5], Chen-Hsi Wang[2], Julianna Gough[2], Sasha Hobson[7], Amanda Deligtisch[5], Gerson Suarez Cedeno[5], Dana Sugar[5] & Sephira G. Ryman[2,5] ✉

A failure of the glymphatic pathway to clear brain byproducts implicated in neurodegeneration may contribute to the pathophysiology of Parkinson's disease. The glymphatic pathway relies on vasomotion (rhythmic constriction and dilation of blood vessels) to drive cerebrospinal fluid through the interstitial space and clear waste from the brain. The current study demonstrated that intermittent hypercapnia, exposure to low levels of CO_2 in ON-OFF cycles, elicited vasomotion-induced cerebrospinal fluid inflow in both healthy controls and individuals with Parkinson's disease. The magnitude of the vasomotion-induced cerebrospinal fluid inflow in patients with Parkinson's disease was reduced relative to healthy controls. However, intermittent hypercapnia, administered in three 10-minute sessions totaling approximately 30 minutes, increased the appearance of total α-synuclein, neurofilament light, glial fibrillary acidic protein, amyloid $\beta_{1\text{-}42}$, amyloid $\beta_{1\text{-}40}$, and phosphorylated tau 217 in the plasma of both healthy controls and individuals with Parkinson's disease. This suggests that intermittent hypercapnia can be used to clear potentially toxic brain byproducts from the brain, highlighting its potential use as a disease modifying treatment.

The misfolding and aggregation of alpha-synuclein (α-synuclein), neuroinflammatory processes, and co-occurring Alzheimer's disease (AD) are key pathological factors contributing to neurodegeneration and cognitive decline in Parkinson's disease (PD)[1–3]. Reduced clearance of interstitial waste by the glymphatic system may lead to aggregation of α-synuclein and a cascade of neuroinflammatory and related processes[4–6]. The glymphatic pathway relies on vasomotion (infraslow, rhythmic constriction and dilation of blood vessels) to drive cerebrospinal fluid (CSF) through the interstitial space and clear waste from the brain[7,8]. As such, augmenting vasomotion may increase clearance of proteins implicated in neurodegeneration and serve as a disease-modifying intervention. Intermittent hypercapnia (exposure to ON-OFF cycles of elevated CO_2), elicits vasomotion. This suggests that, if systematically applied, intermittent hypercapnia may potentially clear waste products from the brain by activating vasomotion and CSF flow.

Alpha-synuclein exists in different conformations under normal conditions, with a balance between unstructured soluble monomeric and tetrameric forms. Failure of α-synuclein clearance disrupts this balance, and α-synuclein aggregates into pathologic oligomers, protofibrils, and fibrils that ultimately form protein inclusions called Lewy bodies[3]. As such, dysfunction of the glymphatic pathway may play a key role in the pathophysiology of PD, as it likely leads to an increase in α-synuclein or a failure to clear its pathogenic forms[6]. Animal studies have shown that blocking CSF influx leads to α-synuclein accumulation, loss of dopaminergic neurons, and

[1]Department of Mathematics and Statistics, University of New Mexico, Albuquerque, NM, USA. [2]Department of Translational Neuroscience, The Mind Research Network, Albuquerque, NM, USA. [3]New Mexico VA Health Care System, Albuquerque, NM, USA. [4]Department of Internal Medicine, University of New Mexico, Albuquerque, NM, USA. [5]Nene and Jamie Koch Comprehensive Movement Disorder Center, Department of Neurology, University of New Mexico, Albuquerque, NM, USA. [6]University Medical Center Groningen, University of Groningen, Groningen, Netherlands. [7]Department of Neurology, University of New Mexico, Albuquerque, NM, USA. ✉e-mail: sryman@mrn.org

an accelerated onset of PD-like symptoms in animals[9,10]. Human studies have suggested that this system is altered in both patients with PD[10–12] and isolated REM sleep behavior disorder (iRBD; considered to be a prodromal cohort)[4,13,14]. The severity of dysfunction is associated with faster deterioration of motor and cognitive symptoms[12,15,16]. Further, it is important to note that the failure of the glymphatic system not only impacts the clearance of α-synuclein, but other proteins and peptides implicated in neurodegeneration in PD, such as amyloid beta (Aβ), hyperphosphorylated tau, glial fibrillary acidic protein (GFAP), and neurofilament light chain (NfL), which are altered in patients with PD and associated with worse outcomes[17–21].

Transport of CSF from the subarachnoid space along periarterial spaces into the interstitial space, where it mixes with interstitial fluid from the brain parenchyma, is referred to as glymphatic 'influx', whereas the transport of the CSF/interstitial fluid and waste products out of the brain tissue is termed 'clearance' or 'efflux'[22]. While there are ongoing investigations over the precise nature of the fluid flow dynamics and pathways[22], vasomotion is a key driver of both influx and clearance[7,8,23], and may be facilitated by norepinephrine[24], cardiac and respiratory cycles[25,26], or neurovascular coupling[27,28]. Our past work has indicated that patients with PD exhibit reduced cerebrovascular reactivity[29,30] - the brain's ability to adjust blood flow in response to a vasoactive stimulus. Hemodynamic cerebral blood flow coupling with CSF inflow[31–33] may reflect a mechanism by which glymphatic clearance is reduced in PD. Prior studies have also demonstrated that medicated[34] and drug-naïve[35] patients with PD exhibit reduced coupling between the (MRI) blood oxygen level dependent (BOLD) signal in the gray matter (GM) and CSF inflow at rest, suggesting that in addition to reduced vasomotion, patients with PD may experience reduced CSF flow in response to vasomotion, further supporting the notion that patients with PD exhibit reduced glymphatic clearance by these mechanisms.

Notably, partial pressure of blood CO_2[36,37] is a potent driver of CSF fluid flow via cerebrovascular activity. The changes in cerebral blood flow (CSF) in response to CO_2 are primarily due to pH-dependent modulation of vascular smooth muscle tone, although complex, bidirectional interactions with the autonomic nervous system and noradrenergic signaling further influence cerebrovascular dynamics[38,39]. Given that past work has demonstrated that CBF is coupled with CSF inflow[31–33], this highlights that CO_2-driven oscillations in CBF can drive CSF flow. A recent retrospective analysis by van der Voort et al. (2024)[40] demonstrated that hypercapnia, but not hyperoxic challenges, lead to an increase in CBF, and that CBF is coupled with CSF flow. Herein, we use the term cerebrovascular activity, measured using magnetic resonance imaging (MRI) BOLD imaging, as a means to quantify the vasomotion in response to intermittent CO_2. The current study builds upon this work by leveraging brief exposures to low levels of CO_2 (intermittent hypercapnia) to first demonstrate that the paradigm can elicit vasomotion-induced CSF inflow. We then evaluated whether CSF inflow is reduced in patients with PD relative to healthy controls (HC) using a ~5-min intermittent hypercapnia paradigm to better understand disease mechanisms in Study 1.

We also evaluated whether intermittent hypercapnia can elicit an increase of peptides and proteins implicated in neurodegeneration in PD in the blood, suggesting possible clearance from the brain in Study 2. Patients with PD and HC underwent an extended intermittent hypercapnia paradigm as well as measurement of plasma levels of total α-synuclein, NfL, GFAP, amyloid $\beta_{1\text{-}42}$ ($A\beta_{1\text{-}42}$), amyloid $\beta_{1\text{-}40}$ ($A\beta_{1\text{-}40}$), and phosphorylated tau (pTau217) at two baselines and three time points after intermittent hypercapnia. While plasma-based biomarkers are typically used as temporally stable markers of neurodegeneration, recent studies have demonstrated time of day effects whereby pTau217, $A\beta_{1\text{-}40}$, $A\beta_{1\text{-}42}$, and NfL increased following the first three hours of sleep, during which slow wave sleep typically occurs[41]. Increased $A\beta_{1\text{-}42}$, pTau181, and pTau217 were observed following a night of sleep[42], and plasma concentrations of neurodegeneration markers were associated with indices of glymphatic and meningeal lymphatic functions[43]. Further, proteins such as GFAP and NfL are both abundant in and highly specific to the brain[44,45]. Together, this supports their use as outcome measures to detect changes in brain-derived proteins and peptides in the blood following intermittent hypercapnia. We hypothesized that patients with PD will exhibit a reduction in intermittent hypercapnia-induced CSF inflow. Additionally, we hypothesized an increase in the clearance of proteins and peptides in response to an extended intermittent hypercapnia paradigm.

Results

Intermittent hypercapnia elicits vasomotion-induced CSF inflow

Study 1 (Fig. 1A) aims to 1) demonstrate that we can elicit vasomotion induced CSF inflow with our intermittent hypercapnia paradigm and 2) evaluate how these mechanisms may be altered in PD. Seventy-three (35 PD and 38 HC) participants underwent clinical assessment and a ~5-min intermittent hypercapnia paradigm while undergoing MRI BOLD. In Study 1, nine participants (5 PD and 4 HC) were removed due to poor exhaled or end tidal CO_2 ($ETCO_2$; expected response pattern not observed, possibly due to poor mask fitting or failure to appropriately target 10 mmHg increase consistently) and 1 additional subject due to excessive motion, resulting in a final study cohort of 63 participants (33 HC, 21 F, 69.64 ± 14.51 (SD) years old; 30 PD, 14 F, 73.57 ± 6.08 years old). Study 2, all participants had good quality data and no participants were removed. Demographic and clinical data are presented in (Table S1); there were no significant differences in age, sex, and education between groups.

BOLD imaging was processed to obtain measurements of cerebrovascular activity and CSF inflow (Fig. 2). Each CO_2 exposure elicits a large-amplitude BOLD signal (reflecting an increase in cerebrovascular activity) followed by a large-amplitude CSF inflow signal (Fig. 3). We calculated the derivative of the GM BOLD signal to evaluate the degree of coupling[31]. As a decrease in GM BOLD is coupled with the increase in the CSF inflow, the negative of the derivative $GM_{d/dt}$ was used. The change in GM cerebrovascular activity (negative $GM_{d/dt}$ BOLD) and CSF inflow is highly correlated across participants, with mean $r = 0.58$ at lag 1.016 s, with 31/33 HC and 25/30 PD having significantly ($p < 0.05$) higher correlation than chance under bootstrap phase shuffling. The degree of coupling (r), optimal lag, and magnitude of response ($\boldsymbol{\beta}$) between the $GM_{d/dt}$ BOLD and CSF inflow did not differ between groups based on permutation testing ($p = 0.454$, $p = 0.114$, and $p = 0.229$, respectively).

Intermittent hypercapnia-induced cerebrospinal fluid flow is reduced in patients with Parkinson's disease

To evaluate whether patients with PD exhibited an altered CSF response, we quantified the coupling (r), magnitude ($\boldsymbol{\beta}$ values), and

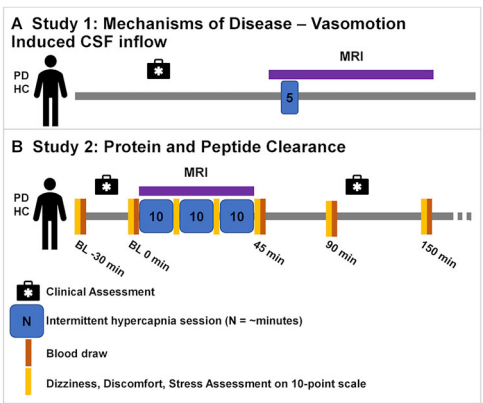

Fig. 1 | Study design overview. A Participants in Study 1 underwent clinical assessments and a ~5-min intermittent hypercapnia paradigm while undergoing MRI BOLD imaging. **B** A subset of these participants was asked to return for Study 2, in which participants underwent three sessions of intermittent hypercapnia (each ~10 min, totaling ~30 min) while undergoing MRI BOLD imaging. An intravenous catheter (IV) was placed to facilitate 5 blood collections: two baselines followed by three post intermittent hypercapnia (~45, 90, and 150 min post *start* of the paradigm). Study 2 also included assessment of dizziness, discomfort, and stress to inform future clinical trials.

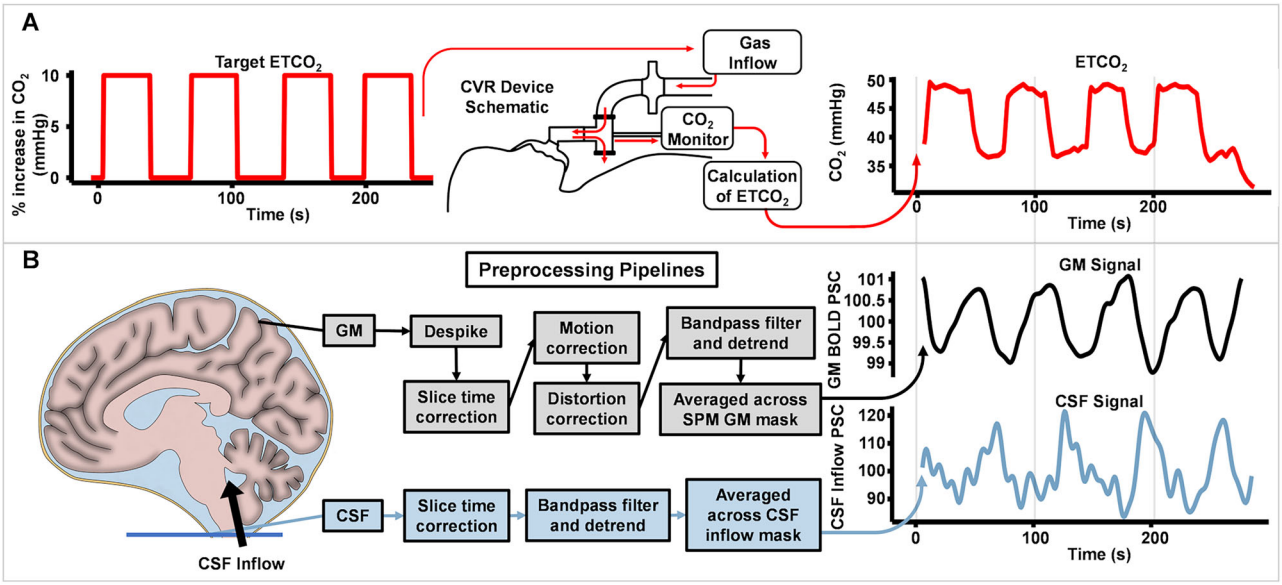

Fig. 2 | Overview of intermittent hypercapnia paradigm and blood oxygen level dependent MRI data processing. A The intermittent hypercapnia paradigm exposes individuals to cycles of 35 s of elevated CO_2 followed by an OFF period (Study 1: 30 ± 5 s; Study 2: 35 s). Exhaled or end-tidal CO_2 ($ETCO_2$) is measured throughout the paradigm, as it closely approximates venous blood entering pulmonary capillary blood levels. $ETCO_2$ is then used to quantify the degree to which cerebrovascular activity and cerebrospinal fluid (CSF) increase in response to $ETCO_2$. Study 1 paradigm is illustrated in which participants underwent 4 cycles of elevated CO_2 in a single session; Study 2 included 24 cycles of elevated CO_2 across three sessions. **B** The overall gray matter (GM) blood oxygen level dependent (BOLD) signal is used to quantify cerebrovascular activity. CSF inflow is detected at the lowest scan slice at the fourth ventricle or central canal as a bright signal (fresh fluid entering the boundary of the imaging volume exhibits high signal intensity since it has not yet been affected by radiofrequency pulses).

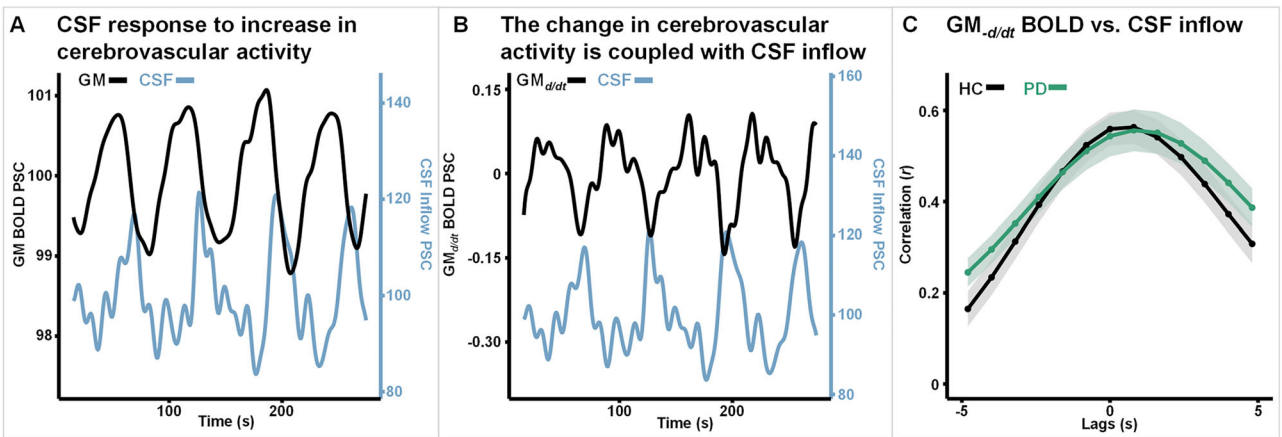

Fig. 3 | Intermittent hypercapnia elicits cerebrovascular activity that is coupled with and drives CSF inflow. A Following intermittent hypercapnia a large-amplitude blood oxygen level dependent (BOLD) signal (cerebrovascular activity) occurs, followed by a large amplitude CSF inflow signal. **B** The change in GM cerebrovascular activity ($GM_{d/dt}$) drives an increase in CSF inflow signal. **C** To verify coupling between the change in GM cerebrovascular activity ($GM_{d/dt}$), we conducted cross-correlations between the -$GM_{d/dt}$ and CSF signals (y-axis) based on the lags in seconds (x-axis), which indicate strong correlations across patients with Parkinson's disease (PD) and healthy controls (HC). The line indicates mean and shaded area corresponds to the standard error of the mean for each group.

lag of the CSF response to intermittent hypercapnia ($ETCO_2$-CSF) and evaluated group differences using permutation testing. Patients with PD exhibited significantly reduced CSF inflow response to $ETCO_2$ (β values) relative to HC ($p = 0.012$; Fig. 4D; Table 1). There were no significant differences between groups in the coupling (r) and optimal lags ($p = 0.704$; Fig. 4D; Table 1) $ETCO_2$-CSF. Consistent with our past reports, patients with PD exhibited a significantly reduced magnitude of GM cerebrovascular activity response (β values) to $ETCO_2$ relative to HC ($p = 0.008$; Fig. 4C; Table 1). Additionally, patients with PD exhibited a significantly delayed GM cerebrovascular response, with optimal lags significantly greater than HC ($p = 0.006$; Table 1).

Intermittent hypercapnia increases clearance

To evaluate whether the extended intermittent hypercapnia paradigm elicited clearance of proteins and peptides implicated in neurodegeneration, five patients with PD and five HCs underwent baseline blood draws followed by an extended intermittent hypercapnia paradigm while undergoing MRI BOLD imaging and subsequent blood draws after intermittent hypercapnia (approximately 45, 90, and 150 min from the start of the paradigm) in Study 2 (Fig. 1B). Demographic and clinical data are presented in Table S2; there were no significant differences in age, sex, or education between groups. Eight out of 10 participants completed the 3 sessions of intermittent hypercapnia, while the other 2 (1 PD and 1 HC) completed 2 of the 3 sessions.

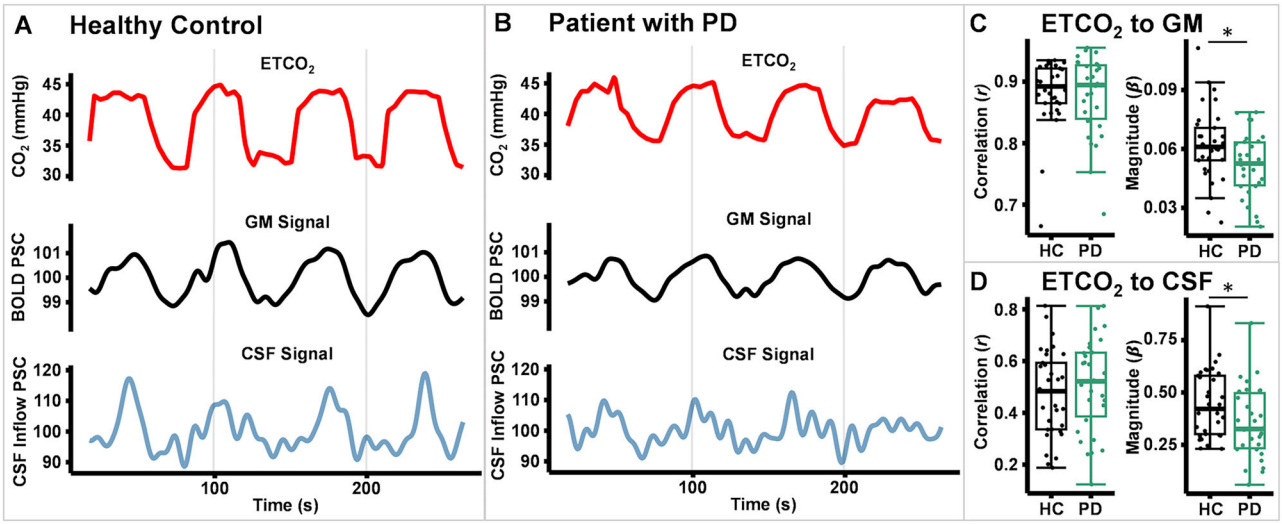

Fig. 4 | Patients with PD exhibit a significantly reduced GM cerebrovascular and CSF inflow response to hypercapnia. A Exemplar healthy control (HC) participant and (**B**) patient with Parkinson's disease (PD). Exhaled or end-tidal CO_2 ($ETCO_2$) reflects the amount of CO_2 that has entered the circulation and is expelled through the lungs. The gray matter (GM) blood oxygen level dependent (BOLD) and cerebrospinal fluid inflow (CSF) signals are presented at the optimal lag from the $ETCO_2$. **C** The correlations (r) reflect the coupling between the $ETCO_2$, GM cerebrovascular activity, and CSF inflow, whereas the β values reflect the magnitude of the GM cerebrovascular activity and CSF inflow in response to $ETCO_2$. Patients with PD exhibit a significantly reduced GM cerebrovascular activity response to intermittent hypercapnia relative to HC. **D** Patients with PD exhibit a significantly reduced CSF inflow relative to HC.

Table 1 | Group differences

Model	Parameter	DX	Estimate	Hypothesis	*p*-value
$ETCO_2$-GM	Correlation	HC	0.882 (0.736, 0.934)	HC > PD	0.381
		PD	0.877 (0.734, 0.952)		
	Lag (s)	HC	13.6 (9.92, 19.4)	HC ≠ PD	0.006
		PD	15.5 (10.3, 19.4)		
	β values	HC	0.0620 (0.0266, 0.0974)	HC > PD	0.008
		PD	0.0518 (0.0222, 0.0784)		
$ETCO_2$-CSF	Correlation	HC	0.476 (0.199, 0.779)	HC > PD	0.772
		PD	0.509 (0.208, 0.807)		
	Lag (s)	HC	32.1 (23.0, 44.2)	HC ≠ PD	0.704
		PD	31.3 (17.4, 43.7)		
	β values	HC	0.448 (0.232, 0.726)	HC > PD	0.012
		PD	0.354 (0.104, 0.661)		
$GM_{cl/dt}$-CSF	Correlation	HC	0.588 (0.245, 0.902)	HC > PD	0.546
		PD	0.580 (0.141, 0.848)		
	Lag (s)	HC	0.80 (0, 2.56)	HC ≠ PD	0.114
		PD	1.25 (0, 4.22)		
	β values	HC	59.8 (23.2, 118)	HC > PD	0.771
		PD	55 (11, 102)		

For each Model and Parameter, the group estimates [mean (equal-tailed bootstrap 95% CI limits)] and permutation test p-values for the a priori hypothesized one-sided or two-sided difference in means.

Table S4 presents the average values of the plasma biomarkers at each time point. One patient with PD exhibited plasma biomarkers suggestive of co-occurring AD pathology ($A\beta_{1\text{-}42}/A\beta_{1\text{-}40}$ ratio = 0.06; pTau217 = 1.17 pg/mL). This individual exhibited a robust increase in plasma $A\beta_{1\text{-}40}$ (30.4%) and $A\beta_{1\text{-}42}$ (11.7%) following intermittent hypercapnia, although they were deemed to be an outlier and excluded from analyses. Linear mixed-effects model analysis[46] evaluating the changes in plasma levels of the proteins and peptides indicated a significant positive effect (increase) in plasma total α-synuclein ($p = 0.02$), NfL ($p < 0.001$), GFAP ($p < 0.001$), $A\beta_{1\text{-}42}$ ($p = 0.046$), $A\beta_{1\text{-}40}$ ($p = 0.035$), with a trend effect observed for pTau217 ($p = 0.097$) following the extended intermittent hypercapnia at the first time point available following the paradigm (~ 45 min from the start of the intermittent hypercapnia; HC = 49.6 ± 3.2 min, PD = 50.8 ± 4.1; Fig. 5; Table 2).

This effect was also significant 90 min post intermittent hypercapnia for GFAP ($p = 0.001$) and NfL ($p = 0.032$), and significant at 150 min for GFAP ($p = 0.024$), whereas the other plasma peptides returned to baseline levels. The observed effect sizes were large for GFAP and NfL [Cohen's $d = 1.84$, 95% CI (1.05, 2.61); and $d = 1.57$, (0.82, 2.31), respectively], with 25.1% (5.1 to 35.9%) and 14.7% (4.8 to 31.1%) increases, on average, for the NfL and GFAP proteins at the 45-min time period, respectively.

Eight/10 and 9/10 individuals exhibited a positive increase in $A\beta_{1\text{-}42}$ and $A\beta_{1\text{-}40}$ relative to baseline, respectively, ranging from 0.3 to 8.7% for $A\beta_{1\text{-}42}$ and 2.5 to 7.8% for $A\beta_{1\text{-}40}$. Seven out of 10 participants exhibited a positive increase in pTau217 ranging from 0.9 to 20%. Effect sizes for the remaining plasma markers were as follows: α-synuclein $d = 0.72$, 95% CI (0.04, 1.39); $A\beta_{1\text{-}42}$ $d = 0.58$, (−0.09, 1.24); $A\beta_{1\text{-}40}$ $d = 0.62$, (−0.05, 1.29); pTau217 $d = 0.44$, (−0.22, 1.10). Given differences in the paradigms used for Study 1 and 2, we have provided the $ETCO_2$ values for each study and group in Table S3.

Intermittent hypercapnia is safe and feasible

We assessed safety and feasibility (measuring acceptability, adherence, and tolerability) during Study 2 to inform the development of future clinical trials. No moderate or severe adverse events occurred. We monitored $ETCO_2$ throughout the intervention, which closely correlates with partial pressure of CO_2 (PaCO), though measurements may typically be 2-3 mmHg lower than $PaCO_2$ (e.g., arterial-to-$ETCO_2$ gradient)[47]. Across the 10 participants in the study, there was no indication of a gradual increase in the baseline or max $ETCO_2$ values across the intermittent hypercapnia sessions. Self-reported dizziness, discomfort, and stress were assessed on a ten-point scale throughout the study visit and immediately following each of the intermittent hypercapnia sessions administered in the MRI and were generally low (Figure S1). Additional details regarding the elevations in individuals are provided (Supplemental Feasibility Results).

Discussion

In this study, we demonstrated that intermittent hypercapnia induced a high amplitude cerebrovascular response, which was followed by a high

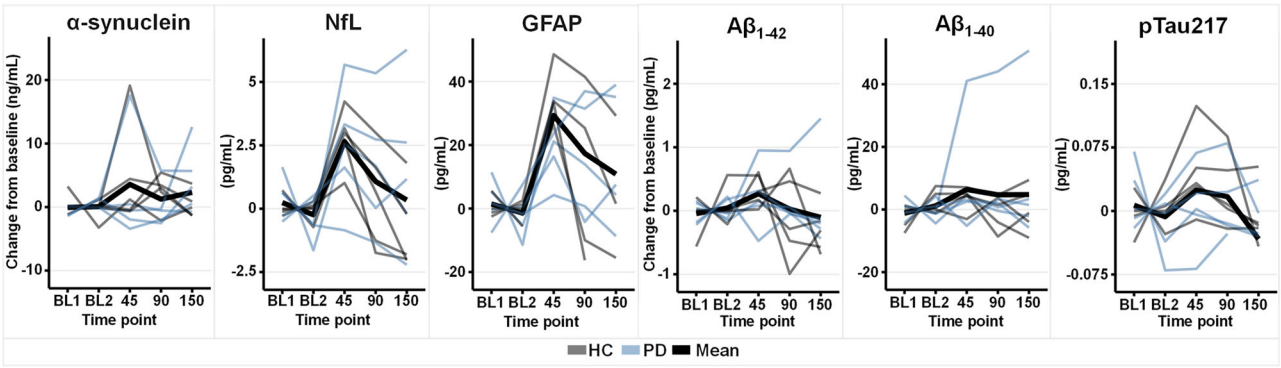

Fig. 5 | Plasma biomarkers in response to intermittent hypercapnia. All plasma biomarkers exhibited an average increase in concentrations following 3 approximately 10-min intermittent hypercapnia sessions. Two baseline (BL) measurements were collected and subsequent measures occurred relative to the start of the intervention (~45, 90, and 150 min post).

Table 2 | Plasma biomarkers increase following intermittent hypercapnia

Plasma Measures	45 min - Baseline	90 min - Baseline	150 min - Baseline
α-synuclein (ng/ml)	3.57 ($p = 0.0189$)	1.25 ($p = 0.2283$)	2.32 ($p = 0.0850$)
NfL (pg/ml)	2.64 ($p < 0.0001$)	1.07 ($p = 0.0317$)	0.34 ($p = 0.2728$)
GFAP (pg/ml)	29.33 ($p < 0.0001$)	17.35 ($p = 0.0012$)	10.82 ($p = 0.0244$)
$A\beta_{1-42}$ (pg/ml)	0.27 ($p = 0.0458$)	0.03 ($p = 0.4335$)	−0.10 ($p = 0.7465$)
$A\beta_{1-40}$ (pg/ml)	6.39 ($p = 0.0354$)	4.69 ($p = 0.0904$)	4.77 ($p = 0.0867$)
pTau217 (pg/ml)	0.02 ($p = 0.0967$)	0.02 ($p = 0.1842$)	−0.03 ($p = 0.9595$)

Contrasts from the linear mixed-effects models indicate significant differences [ng/ml or pg/ml (p-value)] following the intermittent hypercapnia (approximately 45 min since the start of the paradigm) relative to baseline measurements averaged across two baseline timepoints. These differences persisted for NfL and GFAP at 90 min post start of paradigm relative to baseline. While it approached baseline, GFAP remained elevated at 150 min post start of paradigm.

amplitude increase in CSF inflow in both HC and patients with PD. Similar to what has been demonstrated in sleep and during resting states[31–33], we verified that these signals were coupled. We demonstrated that vasomotion-induced CSF inflow was reduced in patients with PD, extending our prior findings that patients with PD exhibit reduced cerebrovascular activity in response to intermittent hypercapnia[29,30]. We showed that three 10-min sessions of intermittent hypercapnia totaling 30 min in patients with PD and healthy controls effectively increased CSF inflow and glymphatic clearance, as evidenced by subsequent concentration increases in total α-synuclein, NfL, GFAP, $A\beta_{1-42}$, $A\beta_{1-40}$, and pTau217 in plasma.

Multiple and likely interrelated factors may lead to a net reduction in glymphatic clearance of waste in patients with PD, including sleep disturbances[4,48], altered autonomic function[49], and altered cerebrovascular activity[6]. Because altered cerebrovascular activity may be evident during the prodromal phases of PD before the appearance of motor symptoms, identifying and treating cerebrovascular reactivity could provide an ideal opportunity to change the trajectory of the disease. Our results highlight the importance of detecting altered cerebrovascular activity early, as a dminished CVR response in our paradigm was closely coupled with an overall reduction in the CSF inflow in patients with PD relative to HC. The observed reduction in CSF inflow was proportional to the magnitude of the reduction in GM cerebrovascular response. This observation, combined with the observed coupling between the GM cerebrovascular response and CSF inflow, suggests that the reduced cerebrovascular activity in patients drives the reduced CSF inflow.

Possible interventions to improve glymphatic clearance of neurotoxins from brain include: (1) pharmacological modulation of noradrenergic tone and aquaporin-4 channels[50] and (2) non pharmacological modulation of body position[51], exercise[52,53], dietary intake of polyunsaturated fatty acids[54,55], and improving sleep quality[56]. Increasing non-rapid eye movement (NREM) sleep duration has been suggested as a potential strategy for increasing glymphatic clearance of neurotoxins given evidence that the glymphatic system is most active when slow wave neural oscillations (< 4 Hz) are present in NREM sleep in both animal[57,58] and human studies[31]. Recent studies showed that ultraslow (~0.02 Hz)[59,60] locus coeruleus (LC)-induced norepinephrine oscillations in NREM sleep were synchronized with cerebral blood volume and CSF inflow, and were the strongest predictors of glymphatic clearance during NREM sleep[24]. This suggests that norepinephrine fluctuations are important for micro-architectural organization of NREM sleep and are a key driver of vasomotion-induced glymphatic clearance during natural sleep.

Instead of depending on NREM sleep to facilitate glymphatic clearance, our intermittent hypercapnia design uses brief exposures to CO_2 (35 s) alternating between CO_2 and OFF periods (either a targeted $ETCO_2$ baseline or room air) to drive vasomotor oscillations. This design allows for the recovery of $ETCO_2$ levels (a full return to baseline), minimizing the potential negative impact of prolonged CO_2 exposures reported in the literature, which do not include opportunities for a return of $ETCO_2$ or partial pressure of CO_2 in arterial blood to baseline. Importantly, the timing of the CO_2 exposures facilitates an increase in cerebrovascular activity (vasodilation) followed by a return of the measured cerebral blood flow response to baseline, which together leads to vasomotion. Our paradigm achieved a nearly oscillatory frequency of ~0.014 Hz of the cerebrovascular activity, similar to oscillations driven by brain norepinephrine levels[24]. The advantage of our approach is that the oscillatory frequency could be set and changed, if needed. Future research could be directed to identify whether there is an optimal frequency that elicits the most robust glymphatic clearance. Notably, prolonged (non-intermittent) hypercapnia has been reported to have the opposite effect of intermittent hypercapnia based on a single animal study[8]. As prolonged hypercapnia leads to a sustained vasodilatory effect, there is limited vasomotion (oscillatory vasodilation and vasoconstriction), which is the crucial and novel mechanism tested in this study for enhancing glymphatic clearance.

While intermittent hypercapnia can be used as a tool to measure the mechanisms by which the glymphatic pathway is altered in PD, we have also demonstrated its potential use as a disease-modifying therapy. We first illustrated that intermittent hypercapnia elicited robust vasomotion-induced CSF inflow. This is an extension of prior studies that indicated coupling between cerebrovascular activity and CSF inflow during sleep and in a resting state when participants undergo imaging while awake, without any task stimulation[31–33]. A prior study demonstrated that a single hypercapnia exposure induced a change in blood flow and corresponding increase

in CSF inflow by administering a 90-s hypercapnic block (+ 10 mmHg from baseline $ETCO_2$) and a progressively increased 120-s hypercapnic ramp (max. +12 mmHg from baseline)[37]. We extended this by demonstrating that each cycle of hypercapnia/normocapnia was followed by a robust increase in CSF inflow, particularly in response to the decrease in CBF. Importantly, we also emphasize the importance of oscillatory changes in CBF that are likely required to facilitate the pumping of CSF from the perivascular into the interstitial spaces, though future work is necessary to evaluate this. Together, this highlights that intermittent hypercapnia can activate key mechanisms involved in glymphatic clearance of brain derived proteins and peptides implicated in neurodegeneration.

There are limited methodologies available to measure clearance or 'efflux' from the brain parenchyma in humans, particularly methods that are safe, repeatable, and noninvasive. The most compelling work has demonstrated that blood levels of gadobutrol mirrored the tracer level in the cisterna magna, verifying the pathway of intrathecal to blood clearance in humans and providing a means to measure the efficiency of the glymphatic pathway[61,62]. Recent preliminary (preprint) evidence has demonstrated the appearance of biomarkers in plasma following sleep[42] with published evidence of elevated plasma biomarkers following slow wave or NREM sleep[41], when the glymphatic system is most active. In Study 2, we showed a clear increase in plasma biomarkers α-synuclein, NfL, GFAP, $A\beta_{1\text{-}42}$, $A\beta_{1\text{-}40}$, and pTau217 following the intermittent hypercapnia paradigm. The pathways by which these neurotoxins are cleared from the brain parenchyma ("efflux") into systemic circulation ("egress") via the glymphatic pathway are still being elucidated. Efflux can transfer solutes to CSF compartments or directly to egress sites, which include via perivenous, white matter fiber tracts, subependymal flow, dural lymphatics, perineuronal pathways along the cranial and spinal nerves, parasagittal spaces, arachnoid villi, and the adventitia of major cerebral vessels[63–65]. However, it is well established that ultimately brain products are cleared into the bloodstream[43,66], suggesting the increases we observe may reflect the clearance of these proteins from the brain into the bloodstream. It is important for future work to rule out other sources, such as blood-brain-barrier leakage or release from peripheral organs. Some evidence suggests blood-brain-barrier failure in patients with PD[67,68], which would suggest that the observed effects may be due to leakage from the interstitial space. However, our results show an effect in PD and HC, suggesting this is an unlikely mechanism. Additionally, hypercapnia can influence blood-brain-barrier permeability, but this has only been demonstrated in the context of hypoxemia and there is limited evidence to suggest that intermittent CO_2 alone would negatively influence the blood brain barrier[69]. The most robust effects were observed in GFAP and NfL, which are CNS-derived, suggesting these changes are not due to release from peripheral organs. However, this cannot be assumed for α-synuclein, $A\beta_{1\text{-}42}$, $A\beta_{1\text{-}40}$, and pTau217, which can be found in peripheral organs and tissues.

We showed a significant overall effect that suggests intermittent hypercapnia can facilitate clearance of total α-synuclein in patients with PD and HC, though the effect was likely driven by a subset of participants and warrants further investigation. Alpha-synuclein has been thought to play a critical role in the pathogenesis of PD[3]. Experimental animal studies have shown that blocking CSF influx[9,10] and meningeal lymphatic drainage[70] lead to α-synuclein accumulation, loss of dopaminergic neurons, and an accelerated onset of PD-like symptoms in animals. While it was initially thought that α-synuclein was an intracellular protein and its pathogenic effects occur within the cell, there is evidence that when misfolding and accumulation occur, its pathological forms can be released into the extracellular space[71], disrupt ingintracellular trafficking and synaptic function, contributing to the formation of Lewy bodies and proinflammatory responses, and leading to prion-like spreading[72]. We also showed increased clearance of NfL and GFAP using intermittent hypercapnia. While α-synuclein is the hallmark pathology of PD, elevations in plasma NfL and GFAP are also strong predictors of cognitive and motor outcomes in PD[17–19]. NfL is a subunit that makes up neurofilaments and, when detected at elevated levels, is thought to reflect neuronal/axonal damage[73]. GFAP is an astrocyte cytoskeletal protein that, when elevated, is thought to reflect astrogliosis[74]. Both of these proteins are highly abundant in the brain, and as such may be particularly useful as targeted outcomes for measuring the efficacy of the glymphatic clearance system. Clearance of these proteins may also be beneficial, as they are implicated in neurodegeneration in PD and, when present intracellularly, may contribute to a pathophysiological cascade.

Increased Aβ and tau co-pathology are strong predictors of worse cognitive outcomes in patients with PD[1,75]. Specifically, approximately 10% of patients with PD and ~35% of PD with dementia patients exhibited Aβ plaques and tau-positive neurofibrillary tangle pathology sufficient for a secondary neuropathological diagnosis of AD[75–77]. One of the participants with PD in our cohort was biomarker positive for AD and exhibited a robust increase in plasma $A\beta_{1\text{-}40}$ (30.4%) and $A\beta_{1\text{-}42}$ (11.7%) following intermittent hypercapnia. As we wanted to evaluate whether there was an effect of intermittent hypercapnia in the rest of the cohort, we excluded this individual from statistical analyses. The responses in the remaining cohort were attenuated, though were statistically significant. This highlights several future directions: (1) intermittent hypercapnia may be able to clear peptides and proteins implicated in AD, highlighting its potential as a disease modifying therapy for AD patients, (2) greater clearance of $A\beta_{1\text{-}42}$ and $A\beta_{1\text{-}40}$ may be more robust in individuals who have evidence of pathology, suggesting an interaction between the abundance of the proteins and peptides in the brain and their clearance.

The current approach only quantifies CSF inflow at the level of the fourth ventricle/central canal, which limits our ability to determine if this increase in CSF inflow translates into an increase in CSF inflow in the perivascular and interstitial spaces. However, moderate hypercapnia elicits marked dilation of the diameter of the cerebral arteries[78] and the arterial wall motion is the principal mechanism driving CSF through the perivascular spaces[23,25,28], suggesting an increase in CSF inflow would correspond to an increase in CSF flow in the perivascular and interstitial spaces driven by vasodilation. This is further supported by our observation of the clearance of brain-derived proteins. However, future direct measurement of CSF in the perivascular and interstitial spaces would be helpful to further demonstrate these mechanisms. Of note, intermittent hypercapnia can be used to elicit changes in the CSF flow as a means to further develop methods to measure tissue CSF flow dynamics.

The technique for administering CO_2 is different across studies. Study 1 targeted a 10 mmHg increase whereas Study 2 used a set mixture of gas that consisted of 5% CO_2, leading to a slightly lower change in $ETCO_2$ in Study 2. The use of different paradigms was primarily due to logistical considerations, as the former approach requires a calibration period between runs, which limited our ability to apply the paradigm for a longer period with brief breaks for check-ins. Based on the mechanisms we propose herein, we would predict that a larger change in $ETCO_2$ would be associated with a larger increase in CBF and corresponding CSF inflow as well as clearance of proteins and peptides implicated in neurodegeneration, though future work is necessary to evaluate this empirically. For Study 1, we lacked systematic field of view placement on the fourth ventricle, which could increase the precision of our measurements and will be incorporated into future studies. This was incorporated in Study 2. All patients were medicated at the time of the scan, suggesting future work should evaluate whether efficacy may differ between medicated and unmedicated patients. Given the small sample size in Study 2, further work is necessary using larger samples to evaluate associations between the mechanisms of action and the changes in plasma biomarkers. Additionally, we were unable to evaluate whether clearance differed by groups, though these data can provide sample size estimates for future studies.

Our findings suggest intermittent hypercapnia can potentially be used as a therapeutic strategy for activating the glymphatic pathway, although the response varied across participants. This highlights numerous future directions. First, it is necessary to compare the clearance of proteins and peptides in response to intermittent CO_2 in a larger cohort of PD patients relative to HC, as we report overall effects across groups in our study. Second, it is important to determine optimal CO_2 concentrations or targeted changes in $ETCO_2$, oscillation frequencies, session durations, and frequency

of administration required to elicit optimal clearance. Third, it is important to recognize that individual differences in physiological responses to intermittent hypercapnia may arise from a variety of factors, such as baseline cerebrovascular reactivity, disease stage, or underlying metabolic states and testing of optimal parameters should incorporate these factors both within and between patient groups to realize the greatest personalized therapeutic potential. Based on the past literature[31], the mechanisms activated by intermittent hypercapnia are similar to what occurs during NREM sleep, though future work should evaluate this empirically and rule out other mechanisms, such as failure of the blood brain barrier and release from peripheral organs. Given that clearance of neurodegeneration-related proteins and peptides typically requires long-term interventions, we anticipate that a single session is likely insufficient, and future work is necessary to determine the necessary frequency of administration to produce clinical efficacy. Future work is also necessary to evaluate how best to use intermittent hypercapnia for clearing different pathogenic forms, whether intermittent hypercapnia-induced clearance is effectively used prophylactically or as treatment, and whether this intervention impacts clinical progression of symptoms. We present initial evidence that intermittent hypercapnia is safe and well tolerated. As the paradigm used in Study 2 is more demanding than what participants would go through when undergoing intermittent hypercapnia as a treatment (e.g., IV placement and participants underwent the paradigm in the MRI whereas if used as a treatment, participants could simply wear a mask). It is therefore necessary to conduct safety and feasibility studies in a more ecologically valid context (e.g., outside of the scanner in a more comfortable environment). Finally, future work can evaluate if intermittent hypercapnia may be useful quantifying the efficiency of the glymphatic pathway as well as elicit clearance as a means to increase sensitivity of blood-based biomarkers by increasing brain-derived proteins in the blood.

Methods

Study design

In this prospective cross-sectional study, we recruited an initial cohort of patients with PD and age- and sex-matched healthy controls for Study 1 and a subset of these participants returned for Study 2 (Fig. 1). All study procedures occurred at the Mind Research Network, in Albuquerque, New Mexico, USA. Recruitment and data collection occurred between February 2021 and February 2025. This study was approved by the University of New Mexico Health Sciences Center Human Research Review Committee. The study was conducted in accordance with the Declaration of Helsinki.

Participants

All subjects were between 50 and 89 years old. Inclusion in the patient group required a previous diagnosis of PD based on the UK Brain Bank criteria. HC were required to have no past or current history of a neurodegenerative condition or evidence of cognitive impairment. Additional exclusion criteria for both groups included: 1) ongoing incarceration, 2) history of a developmental (excluding ADHD), neurological, or serious mental health disorder before the onset of PD (after PD onset was not exclusionary), 3) history of moderate or severe traumatic brain injury, 4) evidence of recent illicit drug use or abuse, 5) estimated IQ < 80 (verified by performance on the Wechsler Test of Adult Reading (WTAR) estimate of premorbid IQ), and 6) contraindications to MRI, including deep brain stimulation. Patients with PD were recruited from the University of New Mexico's Comprehensive Movement Disorders Center. Participants provided written informed consent.

Clinical assessments

Clinical characteristics (Movement Disorders Society Unified Parkinson's Disease Rating Scale[1] Part 3 total score [MDS-UPDRS P3], PD disease duration [age of symptom onset and diagnosis], and levodopa equivalent daily dose[2]) and demographic information (age at baseline, age at symptoms onset, years of education, and sex) were assessed.

Procedure overview

Participants underwent comprehensive clinical and neuropsychological assessments as part of Study 1, though only assessments central to characterizing the cohort are reported (Supplemental Clinical Assessments). As the aim of Study 1 was to evaluate whether 1) intermittent hypercapnia can elicit vasomotion induced CSF inflow and 2) CSF inflow is reduced in patients with PD relative to HC, participants underwent a ~ 5 min intermittent hypercapnia paradigm while undergoing MRI BOLD imaging, which we have previously reported on[29]. Study 2 invited a subset of participants to return to undergo an extended intermittent hypercapnia paradigm (three ~10-min sessions) while also undergoing MRI BOLD imaging. Participants underwent intravenous (IV) catheter placement at the beginning of the Study 2 visit, followed by blood sample collection at five predetermined time points: two baseline time points, immediately after completing the extended hypercapnia paradigm (~45 min), and at 90 and 150 min following the initiation of the hypercapnia paradigm to evaluate whether intermittent hypercapnia can increase the clearance of peptides and proteins implicated in neurodegeneration into the blood (see Fig. 1B). All study visits were conducted in the early afternoon (between 12:00 and 14:00) to control for potential diurnal variation in blood samples, particularly for measuring protein clearance.

Intermittent hypercapnia paradigms

Both intermittent hypercapnia paradigms exposed individuals to 35 s ON periods of low levels of CO_2 followed by OFF periods (Study 1 included 4 cycles in a single session, OFF periods 30 ± 5 s; Study 2 included 24 cycles across 3 sessions, OFF periods consistently 35 s). $ETCO_2$ is measured throughout the paradigm as it closely approximates venous blood entering pulmonary capillary blood levels[79] and can be used as a safety measure and to characterize the cerebrovascular activity and CSF response to the degree of $ETCO_2$ in subsequent analyses. Study 1 used the RespirAct™ system (Thornhill Research Inc. Toronto, Canada), which includes a period of calibration followed by precisely controlled breath-by-breath inhaled gas concentrations aiming for a 10 mmHg $ETCO_2$ pressure increase above the individual's baseline during wakefulness[80] based on the individual's $ETCO_2$ (Fig. 2A). In between CO_2 exposures (OFF periods), participants were exposed to a gas mixture that targets the subject's baseline $ETCO_2$. Given the Respiract requires a ~5-min calibration period before each session, it was not feasible to use for Study 2 and we used a Douglas bag to deliver a medical grade gas mixture (5% CO_2, 21% O_2, balance Nitrogen) for 35 seconds at a time (ON period) alternating with room air for 35 s (OFF period). 5% CO2 was used as this has been routinely used in past studies to evaluated cerebrovascular reactivity[81]. The length of the intermittent hypercapnia paradigm for Study 2 (3 sessions approximately 10 min each) was chosen based on the following: (1) NREM N3 sleep cycles are typically ~20–40 min in length and thus we aimed for a similar timeframe (30 min overall), (2) we anticipated 30 min of continuous fMRI scanning would not be feasible in this population and thus administered three ~10 min sessions with brief breaks to check in with the participant. During Study 2, $ETCO_2$, electrocardiogram (ECG), and oxygen saturation (SPO_2) were measured using the BIOPAC Systems (MP200 Data Acquisition with AMI100D Module), CO_2 Measurement Module; ECG Amplifier, C Series; and Human SPO_2 Module, respectively.

Neuroimaging acquisition and processing

All MRI data were collected using a Siemens PRISMA fit 3 T MRI scanner and preprocessed based on past publications. T1-weighted images were collected using either a five-echo MPRAGE sequence [TE (echo time) = 1.61, 3.47, 5.33, 7.19, and 9.05 ms, TR (repetition time) = 2.53 s, TI (inversion time) = 1.2 s, 7° flip angle, NEX (number of excitations) = 1, FOV (field of view) = 256 mm, and voxel size = 1.0 × 1.0 × 1.0 mm] (Study 1: 44 subjects, Study 2: 10 subjects) or the four-echo Human Connectome Project (HCP) sequence [TE = 1.81, 3.6, 5.39, and 7.18 ms, TR = 2.5 s, TI = 1 s, 8° flip angle, NEX = 1, FOV = 256 mm, voxel size = 0.8 × 0.8 × 0.8 mm] (Study1: 19 subjects, Study 2: 0 subjects). The HCP Aging protocol was used

for functional data collection[3] [TE = 37 ms, TR = 800 ms, 52° flip angle, NEX = 1, FOV = 208 mm, and voxel size = 2.0 × 2.0 × 2.0 mm, 72 slices, multiband acceleration factor = 8].

Vasomotion was measured using BOLD signal changes and referred to as cerebrovascular activity. CSF inflow is detected at the lowest scan slice at the ventricle or central canal as a bright signal (fresh fluid entering the boundary of the imaging volume exhibits high signal intensity since it has not yet been affected by radiofrequency pulses) based on prior publications[31]. Voxelwise gray matter (GM) and CSF time series were obtained in acquisition space by averaging across GM and CSF masks separately to produce individual time series.

Preprocessing. Imaging data were processed using a combination of AFNI[4], ANTS[5], FSL[6], and SPM12[7] software. All images were assessed for quality by two independent raters; poor-quality images were excluded from further analysis. T1-weighted images were cropped (3dAutomask) and then underwent brain extraction (antsBrainExtraction) before undergoing tissue segmentation (SPM12). To create a tissue mask, a 60% threshold was applied to the GM SPM tissue probability maps.

GM processing. GM time-series data were processed similarly to prior publications[8,9] and recent efforts[10–12]. Briefly, functional data were despiked (3dDespike), time-shifted (3dTshift), and registered to the single-band reference image (SBRef) in both 2D (2dImReg) and 3D (3dvolreg) using AFNI. FSL's topup was then used for distortion correction. Distortion-corrected SBRef data were then aligned to the subject's T1 (FLIRT Brain Boundary Registration), and the resulting inverse warp was applied to the GM tissue mask. The first 6 TRs (4.8 seconds) were removed from BOLD data to permit for T_1-equilibrium. A bandpass filter (0.01 to 0.10 Hz) and detrending were simultaneously applied (3dTproject) to the BOLD data.

CSF processing. To replicate previous publications[10–12], CSF time series were processed using only time-slice correction (3dTshift), bandpass filtering (0.01 to 0.10 Hz), and detrending (3dTproject). To identify the fourth ventricle or central canal regions of interest (ROIs), a semi-automated process was used and adjusted per participant if it failed. First, the brain-extracted SBRef image was used to generate the CSF tissue estimates (FSL's FAST) on the most inferior acquired slice and a 0.9 threshold was applied. Visual assessment identified the tissues estimate that corresponded to the fourth ventricle or central canal. The identified tissue had the bottom two slices isolated, and clustered, and the largest cluster was selected. Two independent raters evaluated the masks and manually edited any that failed quality control. Masks were compared among raters until a minimal dice coefficient of 0.70 was obtained (though average dice coefficient = 0.847).

For Study 1, we obtained measurements of the GM response to hypercapnia ($ETCO_2$-CSF), CSF response to hypercapnia ($ETCO_2$-CSF) and the coupling between the GM and CSF ($GM_{d/dt}$-CSF). We scaled each time series to percent signal change. The temporal derivative of the GM was obtained using central finite difference coefficients with accuracy 8 and forward/backward coefficients for boundary points ($GM_{d/dt}$). Cross-correlations between the following variables were computed to identify the optimal lag (the maximal Pearson correlation between pairs of variables; second variable lags behind the first): (1) $ETCO_2$ vs CSF (lags ranging from 8 to 48 s) and (2) -$GM_{d/dt}$ vs CSF (lags ranging from 0 to 5 s based on reported delays ranging from 1.8 to 2.2 s in the literature[31,32]; ranges were visually evaluated to confirm peaks were within the observed windows).

We then aligned the time series by shifting the second variable based on the optimal lag and calculated the correlation to quantify the degree of coupling. Second, we use a simple linear regression predicting the lagged second variable from the first to obtain $\boldsymbol{\beta}$ slope values to quantify the magnitude of the response. Additional analyses verified that $GM_{d/dt}$ is coupled with CSF inflow.

Plasma biomarkers

Blood samples were collected in 10 mL EDTA tubes, centrifuged (1500 g, 15 min, 4 °C) within an average of 5 min post-collection (maximum delay of 12 min), plasma was aliquoted and stored at −80 °C until analysis. Plasma analyses were conducted at the University of New Mexico, and all samples had not previously undergone a freeze-thaw cycle. The Invitrogen Human α-synuclein ELISA Kit (Invitrogen Corporation, ref. KHB0061) was run using freshly thawed plasma aliquots following the kit-specific protocol provided by Invitrogen using the BioTek Synergy H1. Samples were diluted at 1:5 using kit-specific diluent. The Simoa Neuro 4-Plex E Advantage Kit (Quanterix, Billerica MA) and the ALZpath p-Tau 217 Advantage PLUS Kit (ALZpath, Carlsbad, CA) were both run on the same day, containing fluid from the same aliquot, performed by the same scientist, following the kit-specific protocol provided by Quanterix. Two replicates were run on all samples, with the exception of 3 baseline samples given space limitations to ensure all samples could be run on a single plate. As we obtained two baseline measurements, we evaluated the coefficients of variation to ensure data fidelity. All coefficients of variation for internal assay controls were below 6%.

Safety and feasibility outcomes

While this study was not a clinical trial, we assessed safety and feasibility in Study 2 to inform future clinical trials evaluating intermittent hypercapnia. Participants were asked to rate their dizziness, stress, and discomfort levels on a scale of 1–10 throughout the study procedures (Fig. S1).

Verify coupling between $GM_{d/dt}$ and CSF inflow

All statistical analyses were subsequently completed in R (4.4.2). Edge artifacts were induced by the filtering approach and images were cropped to remove these prior to analyses. We compared the observed lagged max cross-correlation to the bootstrapped time series with phase permutation null distribution for a within-subject analysis; roughly described, a time series phase permutation consists of calculating the fast Fourier transform (FFT), permutating the FFT phase coefficients, calculating the inverse FFT of the product of the amplitude times the exponential of imaginary constant i times the permutated phase, and finally retaining the real part to give a new time series where the frequency phases have been shifted -- the two resulting time series have the same frequency information but any synchronicity has been randomized.

Patient-group hypothesis tests between PD and HC use permutation tests on the correlation coefficients (coupling), lag at max correlation, and $\boldsymbol{\beta}$ values (magnitude of response). Linear mixed effects modeling was used to assess blood measures over time adjusted for $ETCO_2$ measures: [blood measure] ~ 1 + timepoint + DX + [$ETCO_2$ measure] + (1 + ID)); where [blood measure] include $A\beta_{1\text{-}40}$, $A\beta_{1\text{-}42}$, α-synuclein, GFAP, NfL, and pTau217; [$ETCO_2$ measure] include corr($ETCO_2$, GM BOLD), $\boldsymbol{\beta}$($ETCO_2$, GM BOLD), corr($ETCO_2$, CSF Inflow), and $\boldsymbol{\beta}$($ETCO_2$, CSF Inflow); and ID are the patient ID numbers as random effects for intercepts. The primary contrasts of interest include the three differences of each follow-up times (45, 90, and 150 min) vs the mean of the two baseline measurements [(BL1 + BL2) / 2].

Data availability

The data generated in this study are available from the corresponding author upon reasonable request.

Received: 30 May 2025; Accepted: 10 October 2025;
Published online: 21 November 2025

References

1. Coughlin, D. G., Hurtig, H. I. & Irwin, D. J. Pathological influences on clinical heterogeneity in Lewy body diseases. *Mov. Disord.* **35**, 5–19 (2020).
2. Hirsch, E. C. & Hunot, S. Neuroinflammation in Parkinson's disease: a target for neuroprotection?. *Lancet Neurol.* **8**, 382–397 (2009).

3. Calabresi, P. et al. Alpha-synuclein in Parkinson's disease and other synucleinopathies: from overt neurodegeneration back to early synaptic dysfunction. *Cell Death Dis.* **14**, 176 (2023).
4. Massey, A. et al. Glymphatic System Dysfunction and Sleep Disturbance May contribute to the pathogenesis and progression of Parkinson's Disease. *Int. J. Mol. Sci.* **23**, 12928 (2022).
5. Sundaram, S. et al. Establishing a framework for neuropathological correlates and glymphatic system functioning in Parkinson's disease. *Neurosci. Biobehav. Rev.* **103**, 305–315 (2019).
6. Ryman, S. G. et al. Abnormal cerebrovascular activity, perfusion and glymphatic clearance in Lewy body diseases. *Mov. Disord.* **39**, 1258–1268 (2024).
7. Iliff, J. J. et al. Cerebral arterial pulsation drives paravascular CSF–interstitial fluid exchange in the murine brain. *J. Neurosci.* **33**, 18190–18199 (2013).
8. Goodman, J. R. & Iliff, J. J. Vasomotor influences on glymphatic-lymphatic coupling and solute trafficking in the central nervous system. *J. Cereb. Blood Flow. Metab.* **40**, 1724–1734 (2020).
9. Cui, H. et al. Decreased AQP4 expression aggravates α-synuclein pathology in Parkinson's disease mice, possibly via impaired glymphatic clearance. *J. Mol. Neurosci.* **71**, 1–14 (2021).
10. Zhang, Y. et al. Interaction between the glymphatic system and α-synuclein in Parkinson's disease. *Mol. Neurobiol.* **60**, 2209–2222 (2023).
11. Shen, T. et al. The role of brain perivascular space burden in early-stage Parkinson's disease. *NPJ Parkinson's Dis.* **7**, 12 (2021).
12. He, P. et al. The Association of the glymphatic function with Parkinson's disease symptoms: neuroimaging evidence from longitudinal and cross-sectional studies. *Ann. Neurol.* **94**, 672–683 (2023).
13. Lee, D. A., Lee, H. & Park, K. M. Glymphatic dysfunction in isolated REM sleep behavior disorder. *Acta Neurol. Scand.* **145**, 464–470 (2022).
14. Bae, Y. J. et al. Altered brain glymphatic flow at diffusion-tensor MRI in rapid eye movement sleep behavior disorder. *Radiology* **307**, e221848 (2023).
15. Park, Y. W. et al. Magnetic resonance imaging–visible perivascular spaces in basal ganglia predict cognitive decline in Parkinson's disease. *Mov. Disord.* **34**, 1672–1679 (2019).
16. Wood, K. H. et al. Diffusion tensor imaging-along the perivascular-space index is associated with disease progression in Parkinson's disease. *Mov. Disord.* **39**, 1504–1513 (2024).
17. Lin, C.-H. et al. Blood NfL: a biomarker for disease severity and progression in Parkinson disease. *Neurology* **93**, e1104–e1111 (2019).
18. Aamodt, W. W. et al. Neurofilament light chain as a biomarker for cognitive decline in Parkinson disease. *Mov. Disord.* **36**, 2945–2950 (2021).
19. Pilotto, A. et al. Plasma NfL, GFAP, amyloid, and p-tau species as Prognostic biomarkers in Parkinson's disease. *J. Neurol.* **271**, 7537–7546 (2024).
20. Batzu, L. et al. Plasma p-tau181, neurofilament light chain and association with cognition in Parkinson's disease. *npj Parkinson's Dis.* **8**, 154 (2022).
21. Chen, N.-C. et al. Plasma Levels of α-Synuclein, Aβ-40 and T-tau as Biomarkers to Predict Cognitive Impairment in Parkinson's Disease. *Front. Aging Neurosci.* **12**, 112 (2020).
22. Benveniste, H. et al. The glymphatic system and waste clearance with brain aging: a review. *Gerontology* **65**, 106–119 (2019).
23. van Veluw, S. J. et al. Vasomotion as a driving force for paravascular clearance in the awake mouse brain. *Neuron* **105**, 549–561 (2020).
24. Hauglund, N. L. et al. Norepinephrine-mediated slow vasomotion drives glymphatic clearance during sleep. *Cell* **188**, 606–622 (2025).
25. Mestre, H. et al. Flow of cerebrospinal fluid is driven by arterial pulsations and is reduced in hypertension. *Nat. Commun.* **9**, 4878 (2018).
26. Helakari, H. et al. Human NREM sleep promotes brain-wide vasomotor and respiratory pulsations. *J. Neurosci.* **42**, 2503–2515 (2022).
27. Murdock, M. H. et al. Multisensory gamma stimulation promotes glymphatic clearance of amyloid. *Nature* **627**, 149–156 (2024).
28. Holstein-Rønsbo, S. et al. Glymphatic influx and clearance are accelerated by neurovascular coupling. *Nat. Neurosci.* **1**, 12 (2023).
29. Ryman, S. G. et al. Reduced and Delayed Cerebrovascular Reactivity in Patients with Parkinson's Disease. *Mov. Disord.* **38**, 1260–1272 (2023).
30. van der Horn, H. J. et al. Parkinson's disease cerebrovascular reactivity pattern: a feasibility study. *J. Cerebral Blood Flow Metab.* **44**, 1774–1786 (2024).
31. Fultz, N. E. et al. Coupled electrophysiological, hemodynamic, and cerebrospinal fluid oscillations in human sleep. *Science* **366**, 628–631 (2019).
32. Yang, H.-C. et al. Coupling between cerebrovascular oscillations and CSF flow fluctuations during wakefulness: an fMRI study. *J. Cereb. Blood Flow. Metab.* **42**, 1091–1103 (2022).
33. Nair, V. V. et al. Neurofluid coupling during sleep and wake states. *Sleep. Med.* **110**, 44–53 (2023).
34. Han, F. et al. Decoupling of global brain activity and cerebrospinal fluid flow in Parkinson's disease cognitive decline. *Mov. Disord.* **36**, 2066–2076 (2021).
35. Wang, Z. et al. Reduced coupling of global brain function and cerebrospinal fluid dynamics in Parkinson's disease. *J. Cereb. Blood Flow Metab.* **43**, 1328–1339 (2023).
36. Wang, Y. et al. Cerebrovascular activity is a major factor in the cerebrospinal fluid flow dynamics. *Neuroimage* **258**, 119362 (2022).
37. van der Voort, E. C et al. CO_2 as an engine for neurofluid flow: Exploring the coupling between vascular reactivity, brain clearance, and changes in tissue properties. *NMR Biomed.* **37**, e5126 (2024).
38. Carr, J. M., Caldwell, H. G. & Ainslie, P. N. Cerebral blood flow, cerebrovascular reactivity and their influence on ventilatory sensitivity. *Exp. Physiol.* **106**, 1425–1448 (2021).
39. Hoiland, R. L., Fisher, J. A. & Ainslie, P. N. Regulation of the cerebral circulation by arterial carbon dioxide. *Compr. Physiol.* **9**, 1101–1154 (2019).
40. van Der Voort, E. C. et al. CO2 as an engine for neurofluid flow: Exploring the coupling between vascular reactivity, brain clearance, and changes in tissue properties. *NMR Biomed.* **37**, e5126 (2024).
41. Della Monica, C. et al. P-tau217 and other blood biomarkers of dementia: variation with time of day. *Transl. Psychiatry* **14**, 373 (2024).
42. Iliff, J. J. et al. The glymphatic system clears amyloid beta and tau from brain to plasma in humans. *medRxiv* 2024–07 (2024).
43. Eide, P. K. et al. Plasma neurodegeneration biomarker concentrations associate with glymphatic and meningeal lymphatic measures in neurological disorders. *Nat. Commun.* **14**, 2084 (2023).
44. Zheng, X., Yang, J., Hou, Y., Shi, X. & Liu, K. Prediction of clinical progression in nervous system diseases: plasma glial fibrillary acidic protein (GFAP). *Eur. J. Med. Res.* **29**, 51 (2024).
45. Gafson, A. R. et al. Neurofilaments: neurobiological foundations for biomarker applications. *Brain* **143**, 1975–1998 (2020).
46. Bates, D., Mächler, M., Bolker, B. & Walker, S. Fitting linear mixed-effects models using lme4. *J. Stat. Softw.* **67**, 1–48 (2015).
47. Bhavani-Shankar, K., Moseley, H., Kumar, A. & Delph, Y. Capnometry and anaesthesia. *Can. J. Anaesth.* **39**, 617–632 (1992).
48. Buongiorno, M. et al. Altered sleep and neurovascular dysfunction in alpha-synucleinopathies: the perfect storm for glymphatic failure. *Front. Aging Neurosci.* **15**, 1251755 (2023).
49. Koep, J. L. et al. Autonomic control of cerebral blood flow: fundamental comparisons between peripheral and cerebrovascular circulations in humans. *J. Physiol.* **600**, 15–39 (2022).
50. Lohela, T. J., Lilius, T. O. & Nedergaard, M. The glymphatic system: implications for drugs for central nervous system diseases. *Nat. Rev. Drug Discov.* **21**, 763–779 (2022).

51. Lee, H. et al. The effect of body posture on brain glymphatic transport. *J. Neurosci.* **35**, 11034–11044 (2015).
52. von Holstein-Rathlou, S., Petersen, N. C. & Nedergaard, M. Voluntary running enhances glymphatic influx in awake behaving, young mice. *Neurosci. Lett.* **662**, 253–258 (2018).
53. He, X. et al. Voluntary exercise promotes glymphatic clearance of amyloid beta and reduces the activation of astrocytes and microglia in aged mice. *Front. Mol. Neurosci.* **10**, 144 (2017).
54. Liu, X. et al. Polyunsaturated fatty acid supplement alleviates depression-incident cognitive dysfunction by protecting the cerebrovascular and glymphatic systems. *Brain, Behav. Immun.* **89**, 357–370 (2020).
55. Ren, H. et al. Omega-3 polyunsaturated fatty acids promote amyloid-β clearance from the brain through mediating the function of the glymphatic system. *FASEB J.* **31**, 282–293 (2017).
56. van Hattem, T. et al. Targeting sleep physiology to modulate glymphatic brain clearance. *Physiology* **40**, 271–290 (2025).
57. Xie, L. et al. Sleep drives metabolite clearance from the adult brain. *science* **342**, 373–377 (2013).
58. Hablitz, L. M. et al. Increased glymphatic influx is correlated with high EEG delta power and low heart rate in mice under anesthesia. *Sci. Adv.* **5**, eaav5447 (2019).
59. Osorio-Forero, A. et al. Noradrenergic circuit control of non-REM sleep substates. *Curr. Biol.* **31**, 5009–5023 (2021).
60. Antila, H. et al. A noradrenergic-hypothalamic neural substrate for stress-induced sleep disturbances. *Proc. Natl. Acad. Sci. USA* **119**, e2123528119 (2022).
61. Ringstad, G. et al. Brain-wide glymphatic enhancement and clearance in humans assessed with MRI. *JCI insight* **3**, e121537 (2018).
62. Eide, P. K. et al. Clinical application of intrathecal gadobutrol for assessment of cerebrospinal fluid tracer clearance to blood. *JCI insight* **6**, e147063 (2021).
63. Louveau, A. et al. Understanding the functions and relationships of the glymphatic system and meningeal lymphatics. *J. Clin. Investig.* **127**, 3210–3219 (2017).
64. Rasmussen, M. K., Mestre, H. & Nedergaard, M. Fluid transport in the brain. *Physiol. Rev.* **102**, 1025–1151 (2022).
65. Proulx, S. T. Cerebrospinal fluid outflow: a review of the historical and contemporary evidence for arachnoid villi, perineural routes, and dural lymphatics. *Cell. Mol. Life Sci.* **78**, 2429–2457 (2021).
66. van Osch, M. J. et al. Human brain clearance imaging: pathways taken by magnetic resonance imaging contrast agents after administration in cerebrospinal fluid and blood. *NMR Biomed.* **37**, e5159 (2024).
67. Lau, K., Kotzur, R. & Richter, F. Blood–brain barrier alterations and their impact on Parkinson's disease pathogenesis and therapy. *Transl. Neurodegener.* **13**, 37 (2024).
68. Al-Bachari, S., Naish, J. H., Parker, G. J., Emsley, H. & Parkes, L. M. Blood-brain barrier leakage is increased in Parkinson's disease. *Front. Physiol.* **11**, 593026 (2020).
69. Liu, X. et al. Hypercapnia exacerbates the blood–brain barrier disruption via promoting HIF-1a nuclear translocation in the astrocytes of the hippocampus: implication in further cognitive impairment in hypoxemic adult rats. *Neurochem. Res.* **45**, 1674–1689 (2020).
70. Zou, W. et al. Blocking meningeal lymphatic drainage aggravates Parkinson's disease-like pathology in mice overexpressing mutated α-synuclein. *Transl. Neurodegener.* **8**, 1–17 (2019).
71. Lee, H.-J., Bae, E.-J. & Lee, S.-J. Extracellular α-synuclein—a novel and crucial factor in Lewy body diseases. *Nat. Rev. Neurol.* **10**, 92–98 (2014).
72. Abeliovich, A. & Gitler, A. D. Defects in trafficking bridge Parkinson's disease pathology and genetics. *Nature* **539**, 207–216 (2016).
73. Coppens, S., Lehmann, S., Hopley, C. & Hirtz, C. Neurofilament-light, a promising biomarker: analytical, metrological and clinical challenges. *Int. J. Mol. Sci.* **24**, 11624 (2023).
74. Yang, Z. & Wang, K. K. Glial fibrillary acidic protein: from intermediate filament assembly and gliosis to neurobiomarker. *Trends Neurosci.* **38**, 364–374 (2015).
75. Ryman, S. G. et al. Cognition at each stage of lewy body disease with co-occurring Alzheimer's disease pathology. *J. Alzheimer's Dis.* **1**, 14 (2021).
76. Irwin, D. J. et al. Neuropathological and genetic correlates of survival and dementia onset in synucleinopathies: a retrospective analysis. *Lancet Neurol.* **16**, 55–65 (2017).
77. Jellinger, K. A., Seppi, K., Wenning, G. K. & Poewe, W. Impact of coexistent Alzheimer pathology on the natural history of Parkinson's disease. *J. Neural Transm.* **109**, 329–339 (2002).
78. Verbree, J. et al. Assessment of middle cerebral artery diameter during hypocapnia and hypercapnia in humans using ultra-high-field MRI. *J. Appl. Physiol.* **117**, 1084–1089 (2014).
79. Slessarev, M. et al. Prospective targeting and control of end-tidal CO2 and O2 concentrations. *J. Physiol.* **581**, 1207–1219 (2007).
80. Fisher, J. A. The CO2 stimulus for cerebrovascular reactivity: fixing inspired concentrations vs. targeting end-tidal partial pressures. *J. Cereb. Blood Flow. Metab.* **36**, 1004–1011 (2016).
81. Liu, P., Jill, B. & Lu, H. Cerebrovascular reactivity (CVR) MRI with CO2 challenge: a technical review. *Neuroimage* **187**, 104–115 (2019).

Acknowledgements

We want to thank the patients and their families who participated in this project. We also want to thank the following individuals who helped make this project a success: Curtis Osbourn, Samuel Miller, Divyasree Sasi Kumar, Tracey Wick, Haleemah Jackson, Cassie Hoskisson, Amari Haner, and Jon Houck. This study was funded by The Laura Ann White Fund Aiding Neuropsychological Research into Lewy Body Dementia and the National Institutes of Health (R03 AG075408, P30 GM122734, P30 AG086404). The funders played no role in study design, data collection, analysis and interpretation of data, or the writing of this manuscript. Dr. Lin's work is supported by the Winkler Bacterial Overgrowth Research Fund.

Author contributions

Conceptualization: S.G.R., H.C.L. Methodology: E.B.E., A.R.M., H.P., F.T.G.S., C.W., J.R.K., N.J.B., P.R.B., J.L.S., E.H.; Investigation: E.B.E., A.R.M., N.A.S., A.A.V., N.H., C.W., J.G., S.H., S.G.R. Visualization: E.B.E., N.A.S., S.G.R. Funding acquisition, Project administration, Supervision: S.G.R. Writing – original draft: E.B.E., H.C.L., S.E.P.R., H.J.H., N.A.S., A.A.V., N.H., C.W., J.G. Writing – review & editing: A.R.M., A.C., H.C.L., J.P., M.G.D., S.H., A.D., G.S.C., D.S.

Competing interests

The authors declare no competing interests.

Additional information

Supplementary information The online version contains supplementary material available at https://doi.org/10.1038/s41531-025-01179-6.

Correspondence and requests for materials should be addressed to Sephira G. Ryman.